Thermal dissociation and desorption of PH_3 on Si(001): A reinterpretation of spectroscopic data

H. F. Wilson,[1] O. Warschkow,[1] N. A. Marks,[1] N. J. Curson,[2] S. R. Schofield,[3] T. C. G. Reusch,[2] M. W. Radny,[3] P. V. Smith,[3] D. R. McKenzie,[1] and M. Y. Simmons[2]

[1]*Centre for Quantum Computer Technology, School of Physics A28, University of Sydney, Sydney, New South Wales 2006, Australia*

[2]*Centre for Quantum Computer Technology, School of Physics, University of New South Wales, Sydney, New South Wales 2052, Australia*

[3]*School of Mathematical and Physical Sciences, University of Newcastle, Callaghan, New South Wales 2308, Australia*

(Received 20 March 2006; revised manuscript received 30 July 2006; published 8 November 2006)

It was recently shown that low-coverage PH_3 dosing of the Si(001) surface is fully dissociative at room temperature with PH_2+H, PH+2H, and P+3H as intermediate species. Here, we consider high-coverage PH_3 dosing and show that the increased density of adsorbates leads to qualitatively different behavior due to competition between thermal dissociation and desorption. Using a combination of existing temperature-programmed desorption data and density functional theory simulations, we present a detailed mechanistic understanding of phosphine adsorption, dissociation, and desorption on the surface. This understanding provides a consistent interpretation of existing infrared and x-ray spectroscopic data, as well as an explanation of the dependence of the phosphorus saturation coverage on dosing conditions.

DOI: 10.1103/PhysRevB.74.195310 PACS number(s): 68.35.−p, 68.37.Ef, 68.47.Fg, 73.20.At

I. INTRODUCTION

The adsorption of phosphine (PH_3) on the Si(001) surface is a reaction of technological significance in the *n*-type doping of silicon by chemical vapor deposition and also in the fabrication of nanoelectronic devices by scanning tunneling microscopy (STM) H lithography.[1–4] The PH_3/Si(001) system has been the subject of numerous studies using experimental methods such as scanning tunneling microscopy,[5–10] temperature-programmed desorption (TPD),[11–15] low-energy electron diffraction, x-ray photoelectron spectroscopy (XPS),[8,9,16] and Fourier-transform infrared spectroscopy (FTIR),[17,18] as well as theoretical modeling.[19,20] However, it is only recently that a detailed understanding of the atomic-scale processes governing this system has begun to emerge. By combining an *ab initio* survey of possible PH_3 dissociation products with high-resolution STM data, we have determined the dissociation pathway for isolated phosphine molecules on the Si(001) surface.[21–23] It was found that PH_3 attaches to one side of a Si-Si surface dimer and dissociates rapidly (on a time scale of seconds at room temperature) to form a single-dimer PH_2+H structure, then more slowly to a double-dimer PH+2H structure and, finally, to a three-dimer P+3H structure. Although this assignment is in full agreement with the STM images, it is in conflict with the previously held view[8,9,16–18] that only PH_3 and PH_2 are present at room temperature, and that PH is not formed. In this paper, we revisit and reinterpret the existing spectroscopic data that led to the PH_3 and PH_2 model and show that a more consistent interpretation of these experiments involves PH_2, PH, and P as majority species.

In order to make this reassignment, we extend our understanding of the phosphine dissociation mechanism gained on low-dosed surfaces to the case of saturation-dosed surfaces. We will show that the complex dose-rate- and temperature-dependent behavior of PH_3 on a highly dosed surface results from competition between three processes: (i) the adsorption of PH_3 molecules onto the surface, (ii) the dissociation of previously adsorbed molecules, and (iii) the thermal desorption of molecular H_2 and PH_3. The competition arises because the first two processes consume bare Si-Si dimers, while the third process creates bare dimers. Our discussion is organized as follows. In Sec. II, we review the relevant experimental and theoretical literature for the PH_3/Si(001) system. In Sec. III, we outline our *ab initio* methodology, which we use to evaluate various possible thermal desorption processes. In Section IV, we compare calculated desorption energies with experimental TPD data and make assignments of the underlying processes for PH_3 and H_2 desorption. In Sec. V, we discuss the TPD assignments in the context of previously published FTIR and XPS experiments and show that a model involving PH_2, PH, and P as majority species can fully explain the observed dependence of the phosphorus saturation coverage upon dosing temperature and pressure. This understanding should be of great assistance in the atomic-scale fabrication of nanoelectronic structures such as Si:P quantum dots and δ-doped layers.

II. BACKGROUND

Numerous studies using a variety of spectroscopies have been reported for the PH_3/Si(001) system, each examining the surface chemistry as a function of various parameters such as temperature, dose rate, and coverage. Despite the wealth of information in these studies, a consistent interpretation of the underlying atomic-scale processes has been lacking. In the following we briefly outline the most important aspects of these experiments. As we will frequently need to refer to these studies, Table I introduces a list of abbreviations.

Yu, Vitkavage, and Meyerson[12] (YVM) examined Si(001) surfaces dosed with PH_3 to saturation at various temperatures. For each temperature, the phosphorus coverage was measured and a TPD spectrum collected. Thermal desorption of PH_3 and H_2 was observed at 548 and 798 K, and the coverage was found to depend strongly on the exposure temperature. Up to 673 K, the coverage was ≈0.3 monolayers (ML), increasing sharply to 1 ML for exposure at 833 K. A

TABLE I. A compilation of spectroscopic experiments relevant to this study. The second column defines the acronyms used in the text to refer to these works. Keywords indicate the primary spectroscopic techniques used.

Authors	Acronym	Keywords
Yu, Meyerson (1984) (Ref. 11)	YM	Auger, TPD
Yu, Vitkavage, Meyerson (1986) (Ref. 12)	YVM	TPD
Colaianni, Chen, Yates (1994) (Ref. 13)	CCY	TPD, EELS
Yoo, Suemitsu, Miyamoto (1995) (Ref. 14)	YSM	TPD
Shan, Wang, Hamers (1996) (Refs. 17 and 18)	SWH	FTIR
Jacobson, Chiu, Crowell (1998) (Ref. 24)	JCC	Auger, TPD
Tsukidate, Suemitsu (1999) (Ref. 15)	TS	TPD
Hirose, Sakamoto (1999) (Ref. 25)	HS	TPD
Lin, Ku, Sheu (1999) (Ref. 8)	LKS	XPS, STM
Lin, Ku, Chen (2000) (Ref. 9)	LKC	XPS, STM
Tsai, Lin (2001) (Ref. 16)	TL	XPS

similar coverage dependence on temperature has also been observed in XPS experiments by Lin, Ku, and Sheu[8] (LKS).

Colaianni, Chen, and Yates[13] (CCY) performed PH_3 exposure at 100 K, and measured the TPD spectrum as a function of coverage. As we will frequently refer to the CCY data in our discussion, we summarize in Table II the temperatures of the principal PH_3 and H_2 desorption peaks. In addition to the major PH_3 and H_2 desorption temperatures, CCY also report minor peaks indicating multiple desorption pathways. As indicated in the table, several of these peaks are observed only at high coverage. CCY also report isotopic exchange experiments from which they conclude that the 635 K peak arises from recombination of PH_x and surface-bound hydrogen.

Tsukidate and Suemitsu[15] (TS) performed repeated cycles of saturation dosing and annealing on the same sample and recorded TPD spectra at each annealing step. By following the H_2 desorption peak over repeated dosing and annealing cycles, they observed that each cycle led to a 25% reduction in the amount of desorbed hydrogen. This was interpreted as showing that phosphorus replaces 25% of the available silicon surface sites and blocks further adsorption.

TABLE II. Tabular summary of the TPD results of Colaianni, Chen, and Yates (Ref. 13) listing the temperatures of the principal PH_3 and H_2 desorption peaks. Samples were all dosed at 100 K and the PH_3 exposure was varied. Temperatures in square brackets refer to TPD peaks which are significantly smaller than other peaks for the same species. We note that the expression of exposure in units of coverage is made by CCY on the assumption that the sticking coefficient remains close to unity as the dose increases. A 0.6 ML exposure actually corresponds to an overdose as the maximum surface coverage is 0.5 ML (see Fig. 2).

Exposure	TPD PH_3	TPD H_2
0.076 ML		770 K
0.15 ML	[485 K], 635 K	[685 K], 770 K
0.30 ML	[485 K], 635 K	[685 K], 770 K
0.60 ML	[485 K], 635 K	[685 K], 770 K

Further TPD experiments were performed by Jacobson, Chiu, and Crowell[24] (JCC), who focussed primarily on the high-temperature desorption of P_2 above 800 K, which will not be considered in this work. Yoo, Suemitsu, and Miyamoto[14] (YSM) and Hirose and Sakamoto[25] (HS) similarly explored the high-temperature regime.

Complementary to the TPD experiments are the FTIR and XPS spectroscopies which probe the species that remain surface bound. Shan and co-workers[17,18] (SWH) used FTIR vibrational spectroscopy to study the surface chemistry of the PH_3/Si(001) system as a function of dose rate, exposure, and temperature. Two sets of peaks are reported in the P-H stretch region which they assign to PH_3 and PH_2. XPS experiments reported by Lin and co-workers[8,9,16] (LKS, LKC, and TL) track phosphorus in three different chemical environments as a function of exposure and temperature. The assignment of these signals to PH_3, PH_2, and P is based directly on the earlier FTIR assignments by SWH.[17] However, as we will show in Sec. V, a more convincing explanation of the FTIR and XPS experiments involves PH_2, PH, and P as the dominant species.

In recent work[21,22] we have used a combination of STM experiments and *ab initio* calculations to identify three common intermediates of PH_3 dissociation on a lightly dosed Si(001) surface as PH_2+H, PH+2H, and P+3H species, respectively. These three structures outline the dissociation mechanism that is shown in Fig. 1. The PH_3 molecule initially binds to one end of a Si-Si dimer and rapidly dissociates at room temperature to form a one-dimer-wide PH_2+H structure. PH_2+H undergoes further dissociation on a time scale of minutes to form a PH+2H structure. In the final dissociation step, a three-dimer-wide P+3H structure is formed in which P occupies an end-bridge site between dimers. Following complete dissociation, P incorporates into the surface layer by ejecting a silicon adatom—this reaction becomes activated at temperatures of around 650 K.[5,26]

In order to understand these various spectroscopies we consider here our dissociation mechanism (Fig. 1) under situations of high coverage. Critical in the interpretation of these experiments is the fact that PH_2+H, PH+2H, and P+3H

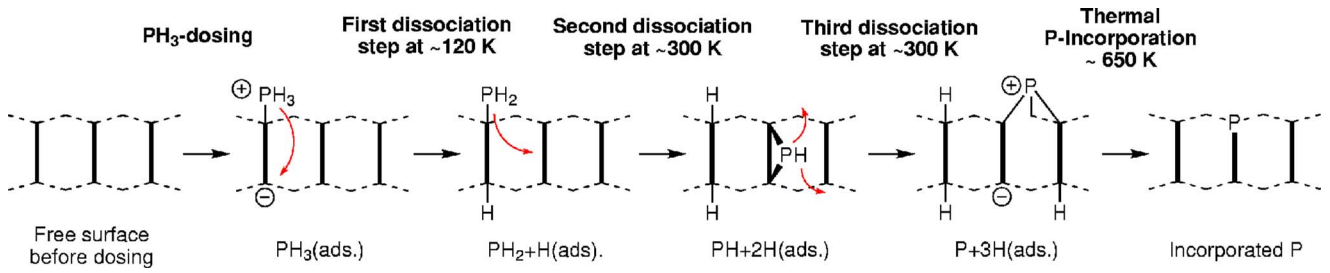

FIG. 1. (Color online) Outline of the dissociation mechanism of low-coverage PH_3 on the Si(001) surface as revealed in previous work using STM images and density functional theory (Ref. 22). Note how the step-by-step dissociation covers an increasing number of surface dimers. As discussed in the text, this is critical to the understanding of the dose-rate dependence of a saturation-dosed surface.

occupy one, two, and three Si-Si dimers, respectively. Thus successive steps in the dissociation pathway lead to the occupation of an increasing number of dimers. If we consider idealized saturation coverages of PH_2+H, PH+2H, and P +3H as shown in Fig. 2, the resulting phosphorus coverage is one-half, one-quarter, and one-sixth of a monolayer, respectively. As we will show below, real surfaces are disordered alloys of these structural units and the precise coverage is dependent on dosing pressure, which determines the rate at which molecules attach to the surface, and the dosing temperature, which determines the rate of dissociation. As shown by CCY,[13] high coverage leads to thermal desorption for which we consider possible mechanisms using *ab initio* methods. It is this combination of desorption and dissociation mechanisms that makes it possible to reintrepret several

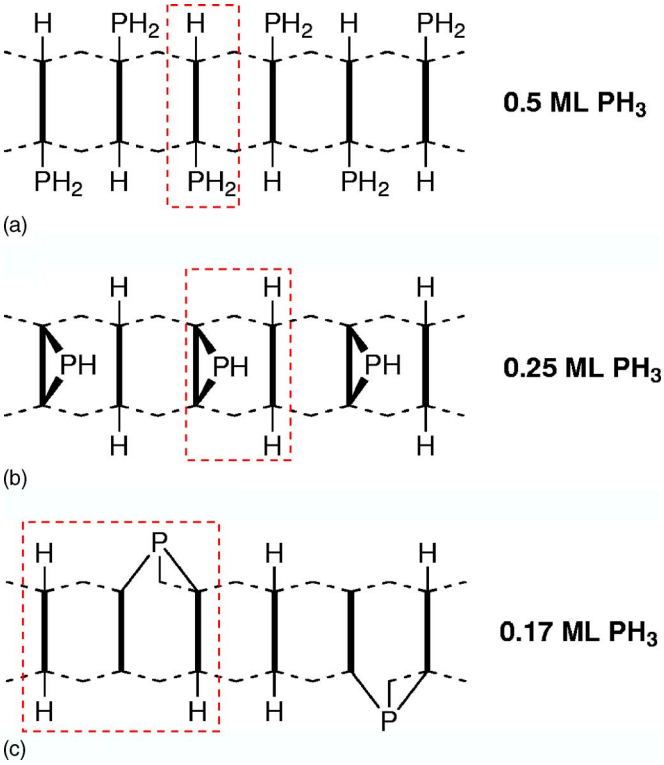

FIG. 2. (Color online) Illustration of surface coverage as resulting from an idealized dense packing of the PH_2+H, PH+2H, and P+3H dissociation intermediates. Note that real coverages are a disordered alloy of these species.

critical assignments and glean important additional insights from existing data.

III. THEORETICAL METHODS

All calculations were undertaken using the plane-wave density functional theory code[27] CPMD in the generalized gradient approximation with the Becke-Lee-Yang-Parr (BLYP) functional.[28,29] The Kohn-Sham equations were solved in a plane-wave basis set with a cutoff of 18 Ry, and core electrons were represented using Goedecker-type pseudopotentials.[30] The Si(001) surface was represented using a slab model with a (4×4) surface unit cell (containing eight Si-Si dimers in two dimer rows) and five Si layers, terminated with a fixed dihydride phase on the lower surface. The vacuum spacing between successive slabs measured 10 Å. All geometric parameters were relaxed except the lowest Si layer and the dihydride termination. The irreducible Brillouin zone was sampled at the Γ point only, which is adequate for the purpose of this work [see Ref. 22, where we tested the accuracy of Γ-point sampling by comparison with a quadruply sized (8×8) surface unit cell].

The objective of these calculations is to determine temperatures at which desorption reactions are activated. The Redhead equation[31] expresses the activation energy for desorption as a function of the thermal desorption temperature and heating rate. In our analysis we use an attempt frequency in the range of $10^{13}-10^{15}$ s^{-1}.[32] Our discussion is based on the CCY data which report the highest-resolution spectra due to the use of a low heating rate (2 K/s).[13] CCY report PH_3 desorption at 485 and 635 K, which correspond to reactions with barriers in the ranges 1.3–1.5 and 1.8–2.0 eV, respectively. H_2 desorption peaks were reported at 685 and 770 K. This corresponds to barriers in the ranges 1.9–2.2 and 2.2–2.5 eV, respectively.

Desorption energies are calculated via three separate geometry optimizations: the surface with the adsorbate, the surface without the adsorbate, and the adsorbate molecule on its own in the gas phase. The desorption energy is then the difference between the energy of the initial adsorbed configuration, and the sum of the energies of the desorbed surface and the free molecule. All sites not involved in the reaction are terminated with hydrogen to emulate a densely covered surface. Tests were performed to confirm that the calculated desorption energies are not sensitive to different

surface terminations involving PH_2+H and PH+2H [Figs. 2(a) and 2(b)]. Note that activation energies for desorption processes will always be higher than or equal to the calculated desorption energies. Thus, using calculated desorption energies as estimates of the activation energies produces lower bounds for activation temperatures.

These lower-bound estimates are sufficient for our purposes as we will be using these energies in conjunction with other sources of experimental and theoretical information. The role of the calculated desorption energies is that of a filter to eliminate processes from our list of prototypical reactions. In the case of the PH_3 desorption reactions, we note that PH_3 adsorption to Si(001) is a near-barrierless process.[20] Consequently, the activation energy of desorption for a surface-bound PH_3 unit is well approximated by the desorption energy. This should apply to all PH_3 desorption reactions considered by us as they are all likely to go through a $PH_3(a)$ intermediate.

IV. RESULTS

A. Assignment of PH_3 desorption peaks

At high coverage, CCY report[13] PH_3 desorption at 485 and 635 K (see Table II). As discussed above, these peaks correspond to reactions with barriers in the ranges 1.3–1.5 and 1.8–2.0 eV, respectively. To assign these peaks we consider a variety of plausible PH_3 desorption reactions shown in Fig. 3. We will address, in turn, prospective desorption reactions involving surface-bound PH_3, PH, and PH_2 species.

The desorption energy for a surface-bound PH_3 [Fig. 3(a)] in our calculations is 0.4 eV, in agreement with similar work by Miotto *et al.*[33] who used a smaller (2×2) cell and found a desorption energy of 0.6 eV. These desorption energies suggest that undissociated PH_3 will desorb at around 120–150 K, which is considerably lower than either of the two PH_3 desorption peaks. The absence of a clear desorption peak at these temperature suggests that most, if not all, PH_3 undergoes dissociation into PH_2+H.[44] This interpretation is supported by theoretical calculations predicting a barrier for the dissociation of PH_3 into PH_2+H that is lower than the desorption energy.[22,23,33,45]

The recombinative desorption of a PH+2H species [Fig. 3(b)] can also be discounted on energetic grounds. The desorption energy for PH+2H is calculated to be 2.9 eV, which translates to a desorption temperature of at least 900 K, far above the observed desorption peaks. Furthermore, the results from TS suggest[15] that an annealed surface with a phosphorus coverage of 0.25 ML [corresponding to a saturation coverage of PH_2+H features; see Fig. 2(b)], does not emit any PH_3 when heated. This indicates that recombinative desorption is not possible once a PH_3 molecule has dissociated to the PH+2H stage. We therefore conclude that the 485 and 635 K PH_3 desorption peaks correspond to two different processes combining a surface-bound PH_2 with a hydrogen atom from elsewhere. In the remainder of this section, we consider possible mechanisms for these reactions.

Recombinative desorption of PH_2 with a hydrogen atom on the same dimer [Fig. 3(c)] has a desorption energy of 2.0 eV which makes this reaction a very plausible candidate for the 635 K peak. In contrast, the sideways recombination of PH_2 with a hydrogen on an adjacent monohydride dimer [Fig. 3(d)] has a desorption energy of 2.4 eV, which is above the expected range for either peak. Since these two reactions have identical starting configurations, the 2.0 eV desorption process [Fig. 3(c)] will be preferred. Recombinative desorp-

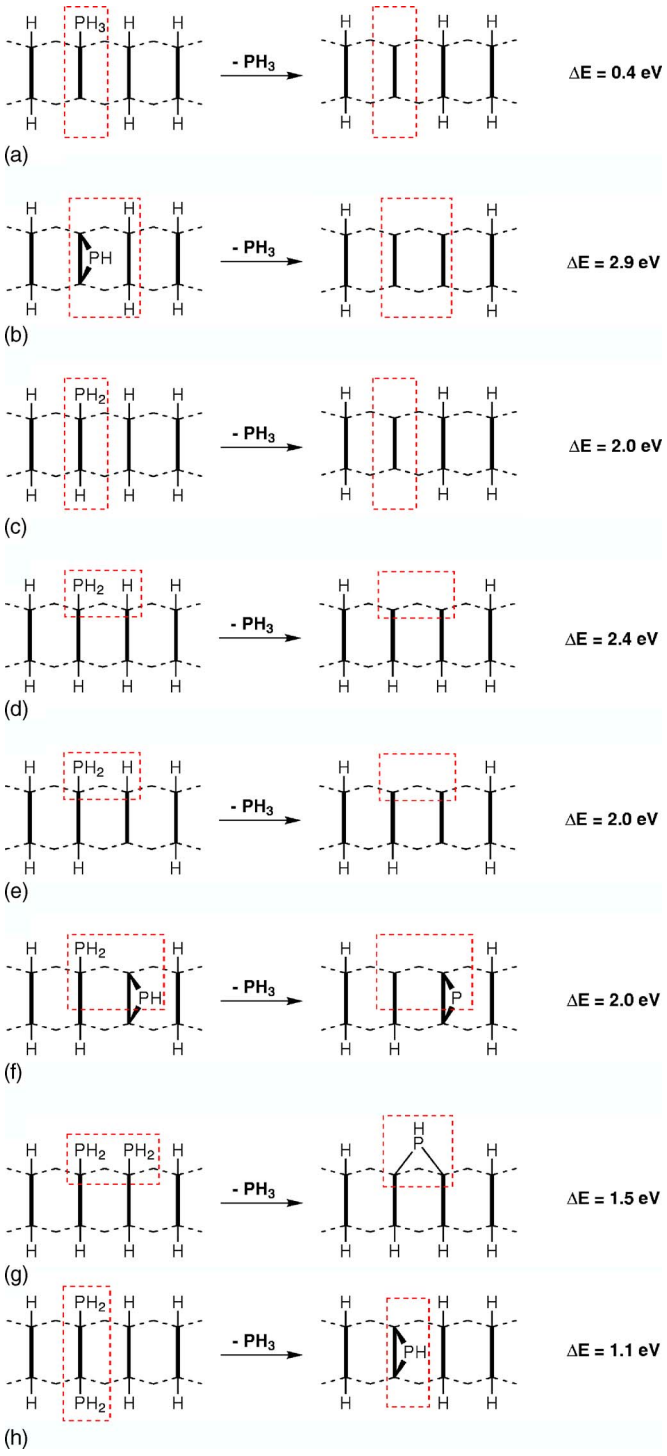

FIG. 3. (Color online) PH_3 desorption processes and energies considered in this work as candidates for the 485 and 635 K TPD peaks.

tion of PH_2 with the H atom of an adjacent hemihydride dimer [Fig. 3(e)] has an energy of 2.0 eV; comparable to the same-dimer recombination [Fig. 3(c)] and thus could conceivably make a contribution to the 635 K desorption.

Before considering additional PH_3 desorption processes, we recall the deuterium-dosing experiments in the CCY work.[13] In these experiments, the surface was exposed to a light dose of deuterium (0.12 ML) prior to phosphine dosing. Subsequent TPD analysis produced singly deuterated phosphine (PH_2D) at the 635 K desorption peak but not at the 485 K peak. CCY conclude that the 635 K peak is due to the recombination of PH_2 with surface-bound H or D.[13] Our calculated desorption energetics for PH_2+H recombination reactions [Figs. 3(c) and 3(e)] support this conclusion. While CCY do not offer an explanation for the 485 K peak, the absence of deuterated phosphine at this temperature suggests that the desorption processes do not involve surface-bound H or D atoms. This leads us to consider recombination reactions of PH_2 in which hydrogen is abstracted from another nearby PH_x species. In Figs. 3(f) and 3(h), three such processes are shown.

Figure 3(f) shows the recombination reaction of PH_2 with the H atom of an adjacent PH group, producing gas-phase PH_3 and a phosphorus adatom. The computed desorption energy for this reaction is 2.0 eV, which discounts this process as an explanation for the 485 K peak (1.3–1.5 eV); however, this reaction might plausibly make a contribution to the 635 K peak.

The reaction in Fig. 3(g) involves two PH_2 species on adjacent dimers. After the recombinative desorption of PH_3, a PH group is left behind which bridges across two dimer ends. The desorption energy for this reaction is 1.5 eV. Figure 3(h) shows the reaction of two PH_2 units on the same dimer, which recombine to form gas-phase PH_3 and a PH dimer bridge with a desorption energy of 1.1 eV. Keeping in mind the possibility of a reaction barrier for these processes, both of these reaction energies are low enough to be consistent with the 485 K desorption (1.3–1.5 eV).

In summary, we confirm the CCY assignment[13] of the major 635 K desorption peak to a PH_2+H recombination reaction. Specifically, the PH_2 group may recombine with either a hydrogen from the same dimer or an adjacent hemihydride. A third possibility involves the abstraction of a hydrogen from an adjacent PH unit. Our calculations show that the minor 485 K peak arises from two PH_2 units, which react to form a PH_3 molecule and a surface-bound PH unit, although we are not in a position to pinpoint the precise reaction pathway.

B. Assignment of H_2 desorption peaks

Desorption of H_2 was observed[13] by CCY at 685 and 770 K. These peaks correspond to estimated activation barriers of 1.9–2.2 eV for the 685 K peak, and 2.2–2.5 eV for the 770 K peak. Notably, the 770 K peak appears independent of PH_3 dose, while the 685 K peak is only seen at higher coverage (0.15 ML and above). Using Gaussian deconvolution of the high-coverage data, we estimate that the 770 K peak accounts for approximately 60% of all H_2 desorbed.

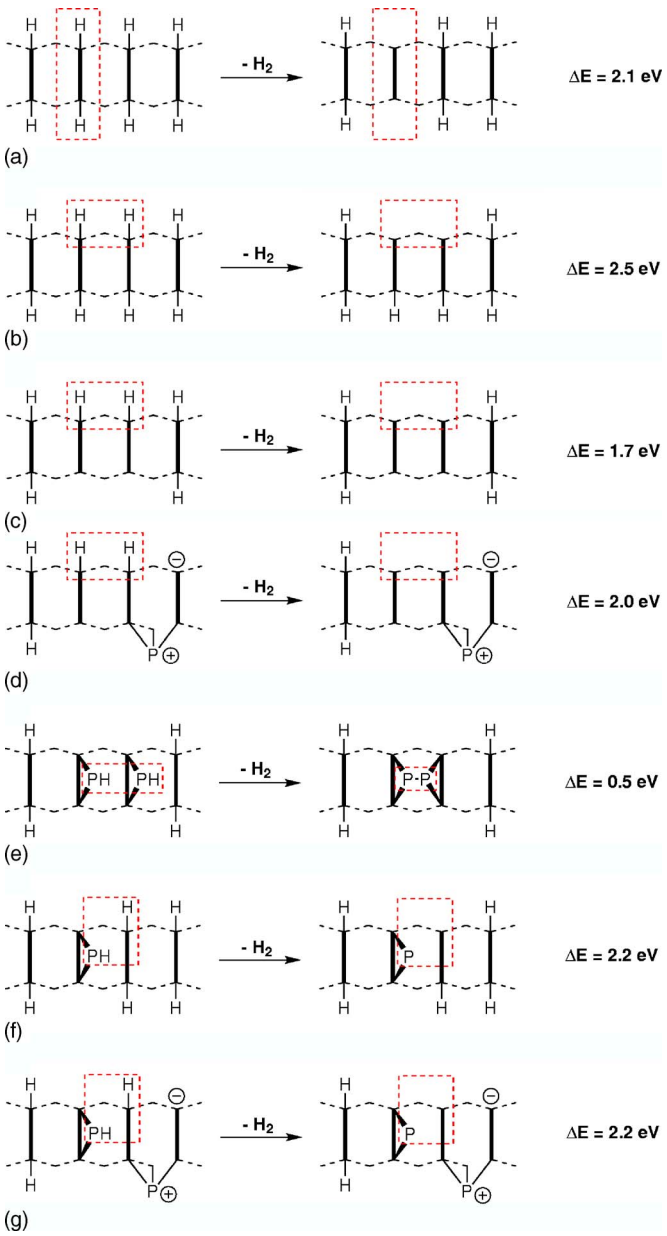

FIG. 4. (Color online) H_2 desorption processes and energies considered in this work as candidates for the 685 and 770 K TPD peaks.

The 770 K peak was assigned by CCY as the β_1 desorption of H_2 from monohydride dimers.[13] Desorption of H_2 in this temperature range is commonly observed following the adsorption of hydrogen-containing species on Si(001).[34–38] The 770 K β_1 desorption process has also been studied extensively using theoretical methods with binding energies reported in the range 1.8–2.0 eV and an activation barrier of approximately 0.3 eV.[39] Our calculated desorption energy of 2.1 eV [Fig. 4(a)] is in good agreement with these works. The additional insight that we provide here is a mechanistic explanation of how the monohydride species are formed. First, the $PH_2+H \rightarrow PH+2H$ dissociation process produces a monohydride as shown in Fig. 1. Second, isolated surface bound hydrogen atoms (such as those found in P+3H structures) become mobile both across and along dimer rows at

≈550 K (Ref. 40) and can pair up to form monohydrides.

It is initially tempting to assign the 685 K peak to β_2 desorption associated with dihydride species (SiH_2) in analogy to similar assignments on Si(001) involving atomic hydrogen,[34–36] disilane,[37] and H_2S.[38] However, the presence of dihydride on the surface in a sufficient quantity to account for this peak appears unlikely, due to the lack of a dihydride signal at any temperature in the FTIR work[17] of SWH on the PH_3/Si(001) system.

Before proceeding any further with an interpretation of the H_2 desorption peak at 685 K, we must first identify which species remain on the surface at this temperature. Since both PH_3 desorption peaks occur at lower temperatures, all remaining structures must be stable with respect to the PH_3 desorption processes discussed in the previous section. This implies that all PH_2+H species have either dissociated into PH+2H, or desorbed as gas-phase PH_3. Furthermore, the onset of the 685 K peak in the CCY experiments[13] for coverages of 0.15 ML and above (see Table II) correlates closely with the maximal ideal coverage of 0.17 ML for full dissociation into P+3H (see Fig. 2). Even considering disordered absorption, at the lowest coverage studied by CCY (0.076 ML) there are sufficient bare dimers available for full dissociation. We can thus conclude that the 685 K peak appearing at higher coverages is associated with inhibited dissociation, and hence the surface at the onset of this peak consists predominantly of PH and monohydrides.

The combination of two hydrogen atoms on adjacent dimers to form gas-phase H_2 is considered in Figs. 4(b) and 4(c). We can immediately discount the H_2 desorption from adjacent monohydrides [Fig. 4(b)] as the energy is significantly higher than in the β_1 process [Fig. 4(a)]. The desorption from adjacent hemihydrides [Fig. 4(c)] has an acceptable desorption energy of 1.7 eV, but this can be discounted because at these temperatures hemihydrides are sufficiently mobile to pair up into monohydrides as discussed previously. A related alternative shown in Fig. 4(d) pairs a hemihydride with a hydrogen opposite a phoshorus in an end-bridge position. Although the desorption energy of 2.0 eV is reasonable, P+3H features are rare in this temperature range and thus unlikely to account for a significant fraction of H_2 desorption.

The combination of two adjacent center-bonded PH species [Fig. 4(e)] has a desorption energy of only 0.5 eV due to the stability gained from the formation of a P-P dimer. Assuming a significant reaction barrier, this process could provide a plausible explanation for the 685 K peak. However, the area of the TPD peaks indicates that approximately 40% of the H_2 desorbs via the 685 K process which would require that all of the PH+2H species are ordered such that all PH units are on adjacent dimers. This situation is not supported by STM experiments,[23] which in fact show that PH+2H features have a tendency to exhibit ordering in which PH and monohydrides alternate [Fig. 2(b)].

The combination of a hydrogen from a PH species with half of an adjacent monohydride species [Fig. 4(f)] has a desorption energy of 2.2 eV which is just within the acceptable range. Since the dissociation of PH_2+H to PH+2H creates a centrally bonded PH unit next to a monohydride, the precursors for this dissociation reaction on the surface should be plentiful. The related variant shown in Fig. 4(g) has the same energy, but as in the case of Fig. 4(d), a lack of bare sites makes this an unlikely explanation for the 685 K peak. Finally, we note that a PH unit adjacent to a hemihydride, i.e.,

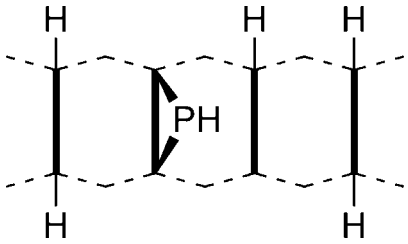

can be immediately discounted as this structure can utilize the dangling bond site and dissociate to form a more stable structure consisting of a phosphorus adatom and a monohydride. This illustrates the earlier point that valid H_2 desorption mechanisms must originate from structures which are stable with respect to onward dissocation. Based on this analysis, we tentatively assign the H_2 desorption peak at 685 K to the combination of hydrogen from a PH unit with hydrogen from an adjacent monohydride [Fig. 4(f)].

V. DISCUSSION

Having considered possible thermal desorption processes for the prominent PH_3 and H_2 peaks, we consider FTIR and XPS spectroscopies to develop an integrated understanding. Expanding on a similar approach by LKS,[8] Fig. 5 presents a correlated overview of various temperature-dependent investigations of the PH_3/Si(001) system. Figure 5(a) summarizes the saturation phosphorus coverage as a function of substrate temperature during exposure,[8,12] while Figs. 5(b) and 5(d) describe experiments in which the surface is PH_3 dosed at low temperature and then heated. It is apparent that sharp changes in the FTIR and XPS spectra are associated with corresponding desorption peaks in the TPD data. In the following, we will reexamine the FTIR and XPS assignments and show that a reinterpretation provides a consistent picture of the PH_3 surface chemistry. This comprehensive understanding allows us to develop an explanation for the temperature dependence of the saturation coverage [Fig. 5(a)]. In particular, we can formulate an intuitive explanation for the 0.25 ML phosphorus coverage typically seen in δ-doped silicon.[41–43]

A. Analysis of FTIR vibrational data

The FTIR[17,18] experiments by SWH examine the temperature dependence of peak intensities in the P-H and Si-H stretch regions for PH_3-dosed Si(001) surfaces. In the P-H region, two groups of peaks are reported: a triplet of peaks at 2268, 2280, and 2290 cm^{-1} (labeled group I) and a group of four peaks between 2239 and 2260 cm^{-1} (labeled group II). SWH assigned these two groups to surface-bound PH_3 and PH_2, respectively, but as discussed by us previously,[22] this assignment is very probably incorrect. The following discussion will be based entirely on our assignment in which groups I and II are PH_2 and PH, respectively. As we show

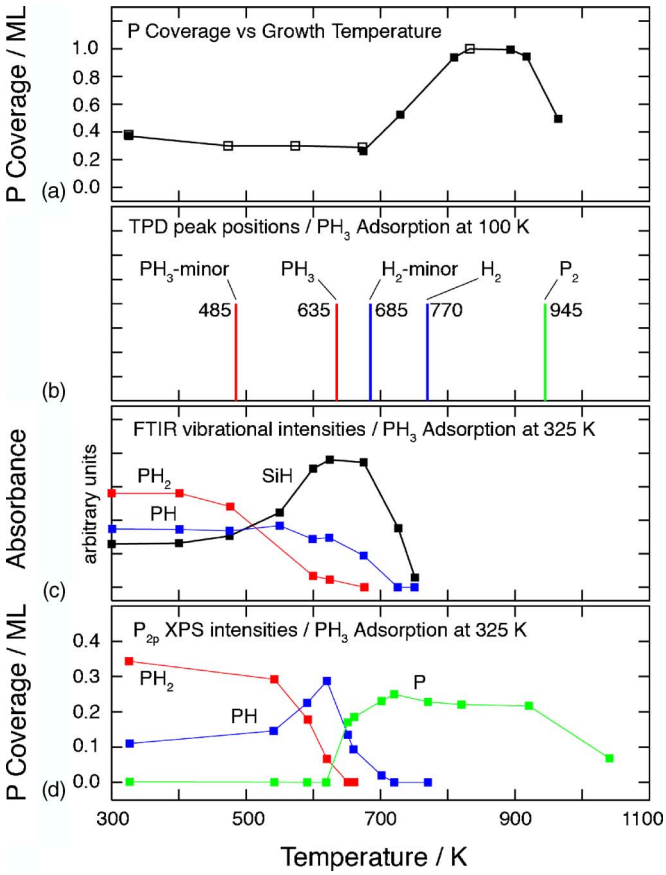

FIG. 5. (Color online) Correlated overview of temperature-dependent spectroscopic data in the literature: (a) Saturation phosphorus coverage as a function of deposition temperature taken from YVM (Ref. 12) (filled squares) and LKS [Fig. 2(a) in Ref. 8, open squares]; (b) TPD desorption peaks for PH_3, H_2, and P_2 taken from CCY (Ref. 13); (c) FTIR temperature dependence of P-H (2245 and 2280 cm^{-1}) and Si-H (2070 cm^{-1}) stretch mode intensities taken from SWH (Fig. 8 in Ref. 17; for clarity, the P-H intensities are scaled by a factor of 3); (d) temperature-dependent phosphorus XPS intensities for room-temperature dosing taken from LKS [Fig. 2(c) in Ref. 8]. Note that the labeling of the data in (c) and (d) as PH_2 and PH indicates the assignments made in this work, which differ from the assignments in the original works.

below, this interpretation provides a more consistent explanation of the thermal and dose-rate dependencies seen in these experiments.

Figure 5(c) shows experimental data[17] from SWH in which the sample was dosed to saturation at a slow rate. These data show the temperature dependence of selected P-H and Si-H peak intensities and tracks the changing abundances of PH_2, PH, and SiH species (our assignments) on the surface. We can explain this behavior by correlation with the H_2 and PH_3 TPD processes discussed in the previous section.

The gradual decline of the PH_2 signal begins with the onset of the 485 K PH_3 desorption peak which removes some of the PH_2 on the surface. According to our assignment [Figs. 3(g) and 3(h)], this initial decline results from the reaction of two PH_2 units in close proximity. At higher temperatures, the 635 K PH_3 desorption process leads to the complete removal of any remaining PH_2 species. The disappearance of PH_2 is due to both thermal desorption as well as the concomitant freeing up of surface dimers which allows other PH_2+H species to dissociate to PH+2H. However, the creation of free surface dimers adjacent to a PH+2H feature may result in its dissociation into P+3H. Thus the observation of constant PH intensity up to a relatively high temperature can be interpretated as a steady-state balance between processes that create and remove PH units. The disappearance of the PH peak around 700 K appears to be associated with the 685 K H_2 TPD peak: this is consistent with our interpretation of this TPD peak as caused by the reaction of PH species with monohydrides [Fig. 4(f)]. The increase of the SiH peak (associated with monohydrides) is anticorrelated with the PH_2 peak, and reflects the increasing number of monohydride species that are formed once space becomes available for dissociation of PH_2+H into PH+2H. The sharp reduction in the SiH peak around 675 K is clearly associated with the onset of the minor H_2 desorption process, and the complete removal of all hydrogen is accomplished once the β_1 temperature of 770 K is reached.

SWH also evaluated the effect of dose rate on the FTIR spectra of saturation-dosed surfaces (see Fig. 3 in Ref. 17). Rapid exposure of the surface (high flux) resulted in increased group I intensities and a slight decrease in group II intensities. This behavior is difficult to rationalize in the original SWH assignment (groups I and II being PH_3 and PH_2+H, respectively) as both species occupy one surface dimer. With our assignment (PH_2 and PH) this flux dependence is naturally explained by the competition between adsorption of PH_3 (which quickly dissociates into PH_2+H), and dissociation of one-dimer-wide PH_2+H into two-dimer-wide PH+2H. Both processes consume free dimers, and thus the relative rates of PH_3 adsorption and PH_2 dissociation determine the balance of the species formed. At high flux the adsorption rate is much greater than the dissociation rate which results in fewer PH species. Conversely, a reduction in flux acclerates the dissociation relative to adsorption, and more PH species are formed. This flux-rate dependence was also observed in our recent STM experiments where a decrease in the dose rate resulted in an increase of PH features at the expense of PH_2 features.[23] An increase in the substrate temperature during dosing was similarly found to increase the amount of PH on the surface. Once more, this can be understood from the perspective of the absorption-dissocation balance, as the higher temperature leads to an acceleration of the dissociation rate.

Additional experiments[17] by SWH were performed in which the surface was not dosed to saturation. For the case of medium coverage (Figs. 3 and 7 in Ref. 17), the PH_2 and PH peaks vanish at 500 and 575 K, respectively. This means that the H_2 desorption processes (685 and 770 K) are not required for full dissociation at medium coverage as sufficient bare dimers are available. In the limit of very low coverage, where the number of bare surface dimers is large, complete dissociation can occur without the need for any desorption processes. This is consistent with the TPD studies[13] of CCY (see Table II) in which the low-coverage experiments did not show any PH_3 desorption.

B. Analysis of XPS experiments

In addition to extensive and detailed STM studies, LKS employed X-ray photoelectron spectroscopy[8] to probe the thermal chemistry of the PH_3-dosed Si(001) surface. These experiments are of particular value because the relative intensities seen in the XPS peaks reflect quantitatively the amounts of phosphorus in three different bonding configurations. LKS assigned[8] these three components to surface-bound PH_3, PH_2 and P, on the basis of the correlation in the temperature dependence of their data and the previous FTIR work by SWH.[17] Our reinterpretation of the FTIR data as showing PH_2 and PH means we must correspondingly reassign the three XPS components as PH_2, PH, and P.

Figure 5(d) shows XPS intensities reported[8] by LKS as a function of temperature. Room-temperature adsorption results in mostly PH_2, some PH, and no P species on the surface. The PH_2 coverage decreases sharply between 550 and 650 K. Over the same temperature range, the PH signal is seen to first double in intensity with a maximum at $\approx$620 K before reducing to zero just above 700 K. The P signal emerges at 650 K and plateaus above 700 K with a 0.25 ML coverage. The decay of the P signal between 900 and 1100 K is clearly correlated with P_2 desorption processes in this temperature range.[13,14,24,25]

While the PH_2 signal is seen to closely mirror the FTIR trend in Fig. 5(c), the initial increase in the PH signal has no correspondence in the FTIR data. The different behavior in the PH signal can be attributed to a higher dose rate in the XPS experiments. This results in a much higher ratio of PH_2 to PH species in comparison to the FTIR experiments. Due to the abundance of PH_2 species, the onset of PH_3 desorption processes creates space that enables other PH_2+H units to dissociate into PH+2H. Since the number of PH species is initially very small, comparatively few PH units can dissociate into P+3H. This bias toward creation of PH units explains the initial increase, and lies in contrast with the FTIR experiments where PH creation and dissociation processes are in balance in this temperature range. Above 620 K the dissociation processes dominate and the decay of the PH signal in the XPS data is similar to that seen in the FTIR experiments.

In another XPS experiment, LKS recorded[8] the room-temperature time evolution of a PH_3-dosed surface exposed to low coverage. Measurements taken at 5 and 30 min after exposure (Fig. 8 in Ref. 8) show an increase of the PH component (our assignment) at the expense of the PH_2 component. This is in full agreement with our recent STM observations which show that PH_2 dissociates to PH on a time scale of minutes at room temperature.[21–23]

C. Coverage vs growth temperature

We now consider Fig. 5(a), which shows the phosphorus saturation coverage as a function of growth temperature. This figure combines the YVM data[12] with the more recent data recorded by LKS.[8] For room-temperature exposure, both sets of experiments report a saturation coverage of $\approx$0.38 ML. As discussed above, room-temperature exposure leads to a flux-dependent balance between PH_2+H and PH+2H species on the surface. An idealized saturation of the surface with PH_2+H species would lead to a total phosphorus coverage of 0.5 ML [Fig. 2(a)]. Similarly, saturation involving PH+2H species only results in a 0.25 ML coverage [Fig. 2(b)]. The observed coverage of 0.38 ML is thus consistent with a mixture of PH_2 and PH species. Dosing at higher temperature accelerates dissociation and the reduction in coverage to a nominal value of 0.25 ML occurs because free surface dimers become more rapidly occupied by expanding dissociation than new adsorption. At a dosing temperature above 700 K, the YVM and LKS data show a sudden increase in phosphorus coverage, which is associated with the desorption of H_2. At this temperature the adsorbed PH_3 molecules fully dissociate into P+3H, phosphorus incorporates into the surface and surface-bound H atoms pair up and desorb as H_2. The latter process frees up surface dimers which enables the adsorption of further PH_3 molecules, leading to higher coverage.

D. Origin of 0.25 ML coverage after annealing

As an application of the chemical understanding presented in this work, we now consider the case of phosphorus δ-doped layers as used in electrical studies of low-dimensional dopant devices in silicon. The STM H-lithographic fabrication of a δ-doped layer typically involves saturation phosphine exposure at room temperature, followed by a high-temperature anneal to incorporate the phosphorus and remove the hydrogen. The phosphorus layer is then encapsulated by depositing additional silicon using molecular beam epitaxy. It is well known that the phosphorus coverage in the plane of the δ doping is independent of the preparation procedure. Regardless of the phosphorus coverage after the room-temperature exposure, the postannealing coverage invariably takes the nominal value of 0.20–0.25 ML.[41–43]

To explain this experimental result, we recall that the phosphorus coverage after saturation dosing (i.e., the PH_2 to PH ratio) reflects the balance between dose-rate- and temperature-induced dissociation. This situation is represented schematically in Figs. 6(a) and 6(b) in which the coverage after room-temperature exposure is a disordered alloy of PH_2+H and PH+2H. We discount the presence of significant amounts of P on the basis of the XPS data [Fig. 5(d)]. Over the course of the anneal, the surface is heated rapidly which activates the 485 and 635 K PH_3 desorption processes. As illustrated in Fig. 6(d), this removes 50% of the PH_2+H units; the remainder can dissociate into PH+2H using the bare surface dimers created in the desorption. In contrast, the PH+2H structures [Fig. 6(c)] remain unaltered in this temperature range. As the annealing process reaches higher temperatures, the H_2 desorption processes at 685 and 770 K are activated. The desorption of hydrogen creates bare dimers which enable the dissociation of PH and the incorporation of the phosporus atom into the surface [Figs. 6(e) and 6(f)]. We thus see that regardless of the initial PH_2 to PH ratio, the final result is a nominal 0.25 ML coverage of phosphorus. The slightly below 0.25 ML coverage (range 0.2–0.25 ML) observed in experiment arises because not all

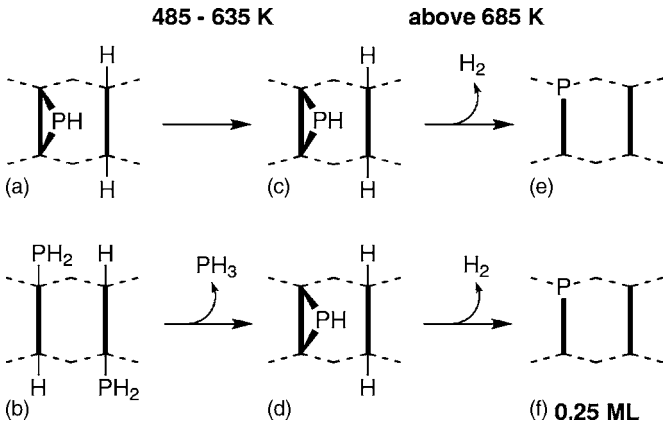

FIG. 6. Schematic explanation of the 0.25 ML phosphorus coverage as observed in experiments involving δ-doped layers (Refs. 41–43). As the annealing temperature rises, the PH_3 and H_2 desorption processes are activated in turn, which removes 50% of all PH_2 units.

PH_2+H units are paired as Fig. 6(b) implies. Leftover single PH_2+H units will become surrounded by PH+2H during the 485–635 K annealing step and, with no space to dissociate into, will desorb as PH_3 as well. As an interesting aside, we note that a higher phosphorus coverage would in principle be possible if H_2 desorption commenced prior to the removal of all PH_3. However, the clear separation between the upper PH_3 peak (at 635 K), and the lower H_2 peak (at 685 K) means that this is not the case. Thus, we only see above 0.25 ML P incorporation in δ-doped layers, when PH_3 dosing is conducted at temperatures above 685 K (when simultaneous H_2 desorption is activated) or, alternatively, when the fabrication involves repeated PH_3 dosing and annealing cycles.

VI. CONCLUSIONS

With the aid of *ab initio* calculations of desorption energies, we have been able to reconcile existing TPD, XPS, and FTIR data on the PH_3/Si(001) adsorption system into a consistent model. PH_3 adsorbs on one side of a dimer and dissociates to form PH_2+H leading to the full occupation of the dimer binding sites. Further dissociation and P-incorporation steps are thermodynamically favored, but will occur only if sufficient bare sites are available on neighboring dimers. In the absence of bare surface sites, molecular desorption of PH_3 from the surface occurs.

Saturation phosphine dosing of the Si(001) surface is dominated by competition between the one-dimer PH_2+H and the two-dimer PH+2H structures. Increasing the dosing rate promotes PH_2+H, while increasing the dosing temperature (up to the limit of hydrogen desorption) promotes PH+2H. Tuning of these parameters results in different mixtures of these two, and the existing spectroscopic data must be analyzed in this context.

Table III presents a summary of critical temperature-activated processes compiled from literature assignments and the interpretations of this work. By providing an overview of the relevant dissociation, desorption, and migration events, this table can be used to interpret processes on the PH_3-dosed Si(001) surface under a variety of conditions. The refined understanding offered by this data should be of considerable utility in the optimization of fabrication processes of *n*-type semiconductors by chemical vapor deposition. Other areas of application include the design of δ-doped layers and protocols for STM H lithography used in the fabrication of atomic-scale electronic devices. Single-dopant placement with atomic precision has recently been demonstrated[3,4] and the detailed understanding of the chemical processes presented here is essential to refine and fine tune this technique.

ACKNOWLEDGMENTS

This work was supported by the Australian Research Council, the Australian Government, the Semiconductor Re-

TABLE III. Approximate temperature of activated surface processes relevant to the PH_3-dosed silicon surface. Bare Si-Si dimers are indicated by a box (□) to highlight their role in the reactions. In the presence of a sufficient number of bare dimers, adsorbed PH_3 will fully dissociate into P+3H at room temperature. Lacking sufficient bare dimers, partial thermal desorption and hydrogen diffusion at higher temperatures create the free dimers required for further dissociation.

Temperature (K)	Process		References
770	H_2 desorption	$H+H \rightarrow \square + H_2(g)$	34 and 35
685	H_2 desorption	$PH+H \rightarrow P+H_2(g)$	
650	H_2 migration	$2H+\square \rightarrow \square+2H$	40
650	P incorporation	P→heterodimer (Si-P)	5 and 26
635	PH_3 desorption	$PH_2+H \rightarrow \square+PH_3(g)$	13
550	H migration	$H+\square \rightarrow \square+H$	40
485	PH_3 desorption	$PH_2+PH_2 \rightarrow PH+PH_3(g)$	
300	dissociation	$PH+2H+\square \rightarrow P+3H$	21 and 22
300	dissociation	$PH_2+H+\square \rightarrow PH+2H$	21 and 22
120	dissociation	$PH_3 \rightarrow PH_2+H$	21 and 22

search Corporation, and the U.S. Advanced Research and Development Activity, National Security Agency, and Army Research Office under Contract No. DAAD19-01-1-0653. Computing support was provided by the Australian Centre for Advanced Computing and Communications (ac3) and the National Facility of the Australian Partnership for Advanced Computing (APAC). M.Y.S. acknowledges financial support from an Australian Government Federation Fellowship.

[1] J. R. Tucker and T. C. Shen, Int. J. Circuit Theory Appl. **28**, 553 (2000).
[2] J. L. O'Brien, S. R. Schofield, M. Y. Simmons, R. G. Clark, A. G. Dzurak, N. J. Curson, B. E. Kane, N. S. Alpine, M. E. Hawley, and G. W. Brown, Phys. Rev. B **64**, 161401 (2001).
[3] S. R. Schofield, N. J. Curson, M. Y. Simmons, F. J. Ruess, T. Hallam, L. Oberbeck, and R. G. Clark, Phys. Rev. Lett. **91**, 136104 (2003).
[4] M. Y. Simmons *et al.*, Mol. Simul. **31**, 505 (2005).
[5] Y. Wang, M. Bronokowski, and R. J. Hamers, J. Phys. Chem. **98**, 5966 (1994).
[6] Y. Wang, X. Chen, and R. J. Hamers, Phys. Rev. B **50**, 4534 (1994).
[7] L. Kipp, R. D. Bringans, D. K. Beigelsen, J. E. Northrup, A. Garcia, and L.-E. Swartz, Phys. Rev. B **52**, 5843 (1995).
[8] D.-S. Lin, T.-S. Ku, and T.-J. Sheu, Surf. Sci. **424**, 7 (1999).
[9] D.-S. Lin, T.-S. Ku, and R.-P. Chen, Phys. Rev. B **61**, 2799 (2000).
[10] N. J. Curson, S. R. Schofield, M. Y. Simmons, L. Oberbeck, and R. G. Clark, Surf. Sci. **532–535**, 678 (2003).
[11] M. L. Yu and B. S. Meyerson, J. Vac. Sci. Technol. A **2**, 446 (1984).
[12] M. L. Yu, D. J. Vitkavage, and B. S. Meyerson, J. Appl. Phys. **59**, 4032 (1986).
[13] M. L. Colaianni, P. J. Chen, and J. T. Yates, Jr., J. Vac. Sci. Technol. A **12**, 2995 (1994).
[14] D. S. Yoo, M. Suemitsu, and N. Miyamoto, J. Appl. Phys. **78**, 4988 (1995).
[15] Y. Tsukidate and M. Suemitsu, Appl. Surf. Sci. **151**, 148 (1999).
[16] H.-W. Tsai and D.-S. Lin, Surf. Sci. **482–485**, 654 (2001).
[17] J. Shan, Y. Wang, and R. J. Hamers, J. Phys. Chem. **100**, 4961 (1996).
[18] R. J. Hamers, Y. Wang, and J. Shan, Appl. Surf. Sci. **107**, 25 (1996).
[19] R. Miotto, G. P. Srivastava, R. H. Miwa, and A. C. Ferraz, J. Chem. Phys. **114**, 9549 (2001).
[20] R. Miotto, G. P. Srivastava, and A. C. Ferraz, Surf. Sci. **482–485**, 160 (2001).
[21] H. F. Wilson, O. Warschkow, N. A. Marks, S. R. Schofield, N. J. Curson, P. V. Smith, M. W. Radny, D. R. McKenzie, and M. Y. Simmons, Phys. Rev. Lett. **93**, 226102 (2004).
[22] O. Warschkow, H. F. Wilson, N. A. Marks, S. R. Schofield, N. J. Curson, P. V. Smith, M. W. Radny, D. R. McKenzie, and M. Y. Simmons, Phys. Rev. B **72**, 125328 (2005).
[23] S. R. Schofield, N. J. Curson, O. Warschkow, N. A. Marks, H. F. Wilson, M. Y. Simmons, P. V. Smith, M. W. Radny, D. R. McKenzie, and R. G. Clark, J. Phys. Chem. B **110**, 3173 (2006).
[24] M. L. Jacobson, M. C. Chiu, and J. E. Crowell, Langmuir **14**, 1428 (1998).
[25] F. Hirose and H. Sakamoto, Surf. Sci. **430**, L540 (1999).
[26] N. J. Curson, S. R. Schofield, M. Y. Simmons, L. Oberbeck, J. L. O'Brien, and R. G. Clark, Phys. Rev. B **69**, 195303 (2004).
[27] J. Hutter, P. Ballone, M. Bernasconi, P. Focher, E. Fois, S. Goedecker, M. Parrinello, and M. Tuckerman, Computer Code CPMD (IBM Zürich Research Laboratory and MPI für Festkörperforschung, 1995–2001).
[28] A. D. Becke, Phys. Rev. A **38**, 3098 (1988).
[29] C. Lee, W. Yang, and R. Parr, Phys. Rev. B **37**, 785 (1988).
[30] S. Goedecker, M. Teter, and J. Hutter, Phys. Rev. B **54**, 1703 (1996).
[31] P. Redhead, Vacuum **12**, 203 (1962).
[32] M. J. Pilling and P. W. Seakins, *Reaction Kinetics* (Oxford University Press, Oxford, 1995).
[33] R. Miotto, G. P. Srivastava, and A. C. Ferraz, Phys. Rev. B **63**, 125321 (2001).
[34] C. C. Cheng and J. T. Yates, Jr., Phys. Rev. B **43**, 4041 (1991).
[35] M. C. Flowers, N. B. H. Jonathan, Y. Liu, and A. Morris, J. Chem. Phys. **99**, 7038 (1993).
[36] S.-S. Ferng, C.-T. Lin, K.-M. Yang, D.-S. Lin, and T.-C. Chiang, Phys. Rev. Lett. **94**, 196103 (2005).
[37] Y. Wang, M. Bronokowski, and R. J. Hamers, Surf. Sci. **311**, 64 (1994).
[38] M. Han, Y. Luo, N. Camillone III, and R. M. Osgood, Jr., J. Phys. Chem. B **104**, 6576 (2000).
[39] E. Pehlke and M. Scheffler, Phys. Rev. Lett. **74**, 952 (1995).
[40] D. R. Bowler, J. H. G. Owen, C. M. Goringe, K. Miki, and G. A. D. Briggs, J. Phys.: Condens. Matter **12**, 7655 (2000).
[41] T.-C. Shen, J. Li, M. A. Zudov, R.-R. Du, J. S. Kline, and J. R. Tucker, Appl. Phys. Lett. **80**, 1580 (2002).
[42] L. Oberbeck, N. J. Curson, M. Y. Simmons, R. Brenner, A. R. Hamilton, S. R. Schofield, and R. G. Clark, Appl. Phys. Lett. **81**, 3197 (2002).
[43] K. E. J. Goh, L. Oberbeck, M. Y. Simmons, A. R. Hamilton, and M. J. Butcher, Phys. Rev. B **73**, 035401 (2006).
[44] Colaianni *et al.* do in fact report in Ref. 13 a broad PH_3 desorption feature at very high exposure. However, they attribute at least part of this signal to desorption from the crystal support assembly.
[45] Reference 23 reports cluster model calculations of PH_3 adsorption and dissociation on an unsaturated Si(001) surface, giving barriers of 0.76 and 0.54 eV for dissociation of $PH_3(a)$ into same-dimer and adjacent-dimer PH_2+H. Using the same computational cluster model, the corresponding desorption energy is calculated to be 0.89 eV (Ref. 22).